Fabrication and photo-electrocatalytic activity of highly oriented titania nanotube loaded with platinum nanoparticles for electro-oxidation of lactose: A new recyclable electro-catalyst

Mir Ghasem Hosseini *, Mohamad Mohsen Momeni

Electrochemistry Research Laboratory, Department of Physical Chemistry, Chemistry Faculty, University of Tabriz, Iran

ABSTRACT

Platinum nanoparticles were doped on TiO$_2$ nanotube arrays (TNT/Ti) by micro-emulsion method. TiO$_2$ nanotube arrays were successfully fabricated by anodizing of titanium sheets. The morphology and surface analysis of Pt/TNT/Ti catalysts were investigated using scanning electron microscopy and energy-dispersive X-ray spectroscopy, respectively. The electro-oxidation of lactose on Pt/TNT/Ti catalysts in alkaline medium was studied by cyclic voltammetry and chronoamperometry methods. The results showed that the oxidation peak currents on the Pt/TNT/Ti catalyst for lactose oxidation are about ten times larger than a smooth platinum electrode and confirmed the better electro-catalytic activity and stability of these new electrodes. The photo-catalytic properties of TiO$_2$ make the Pt/TNT/Ti catalyst refreshable after a short UV treatment and the electro-oxidation current density of Pt/TNT/Ti catalysts after UV-cleaning can be re-established. Also Pt/TNT/Ti catalysts showed a remarkably enhanced performance for lactose oxidation under UV illumination compared to that without UV illumination.

© 2011 Elsevier B.V. All rights reserved.

1. Introduction

As our fossil raw materials are irrevocably decreasing and as the pressure on our environment is building up, the progressive changeover of chemical industry to renewable feed stocks for their raw materials emerges as an inevitable necessity [1]. Direct electrochemical oxidation of carbohydrates is of a very high interest from several points of from biomedical applications involving blood sugar analysis and fuel cells applications [2–6]. The particular interest lays in the alkaline fuel cells applications where the focus was on developing new electro-catalytic materials as platform to carry out the oxidation of fuels, in this case carbohydrates in order to obtain a very high current density [7]. Great efforts have been made to develop catalytically active electrode materials in the past two decades. Various authors have shown that various carbohydrates can be oxidized directly at a variety of electrode materials, including metals such as platinum [8,9], gold [9,10], copper [9,11–13], indium [12], rhodium [12], nickel oxide [14], tungsten oxide [15] and ruthenium oxide [16]. However, systematical study showed that these electrodes were subject to serious poisoning due to adsorbed intermediates from the oxidation of carbohydrates [17]. To mitigate the poisoning effect, significant attention has been focused on

preparing new electrodes with high electro-catalytic activity. For a good electro-catalyst, both the high catalytic activity and the low cost must be considered to meet the final purpose of wide commercialization of fuel cells. High surface area electro-catalytic catalysts are of interest for fuel cell technology. The high surface area electro-catalysts can be made by sintering, electroplating or dispersion of active electro-catalytic materials on a proper support with a relatively high surface area. In searching for novel and stable support for the noble metal catalysts, TiO$_2$ nanotubes come into sight because of their good physical and chemical properties and high stability in acidic and alkaline solutions. Titanium dioxide nanotubes are very biocompatible, inexpensive and environmentally benign [18,19]. Titanium dioxide nanotube arrays have demonstrated a number of important applications including gas sensors, solar cells, photo-catalysts, tissue engineering, biosensors and electro-catalyst [20–23]. TiO$_2$ nanotubes can be synthesized by different methods including sol–gel, hydrothermal, template and anodic oxidation [23–29]. Obviously, if TiO$_2$ nanotubes can be directly produced on a metallic titanium substrate by the anodic oxidation method, it would be advantageous and convenient for fuel cell applications where an electric current collector is required. Moreover, the morphology and the structure of the TiO$_2$ nanotubes layer can also be easily modulated by changing the anodic oxidation conditions [30]. Our recent studies have shown that the immobilization of the metal nanoparticles in a porous matrix improves the electro-catalytic activity to a great extent [31–35]. In this work, a new

* Corresponding author. Tel.: +98 4113393138; fax: +98 4113340191.
  E-mail address: mg-hosseini@tabrizu.ac.ir (M.G. Hosseini).

electro-catalyst for electro-oxidation of lactose in alkaline medium was studied. Lactose is a disaccharide sugar that is found most notably in milk and is formed from the condensation of lactose and glucose, which form a β-1 → 4 glycosidic linkage. Its systematic name is β-D-galactopyranosyl-(1 → 4)-D-glucose. Lactose makes up around 2–8% of milk (by weight), although the amount varies among species and individuals. To the best of our knowledge, the electro-oxidation of lactose is only reported in one article in the literature [36]. Recently photo-electrooxidation of different alcohols and some compounds has been studied thoroughly [37–40]. But to the best of our knowledge, carbohydrates electro-oxidation with assistance of UV illumination is not reported in the literatures. In this context, for the first time, we used from micro-emulsion method to coverage of TiO_2 nanotubes with platinum nanoparticles and tested it as a new electro-catalyst for lactose oxidation in alkaline medium. The surface morphology and element analysis of platinum coating on TiO_2 nanotubes were characterized by scanning electron microscopy (SEM) and energy-dispersive X-ray spectroscopy (EDX), respectively. Due to the large surface area, good electrical conductivity, and unique photo-catalytic properties of TiO_2 nanotube, the resultant Pt/TNT/Ti catalysts not only have high catalytic activity, but also have self-cleaning ability which gives them a reusable feature. The same technique can be employed to prepare electro-catalysts with excellent electro-catalytic activity and refreshable property for lactose electro-oxidation.

2. Experimental

2.1. Chemicals, solutions and equipment

Lactose (Merck, 99% purity) and ethylene glycol (Merck, 99% purity) were used as received. Hexachloroplatinic acid (98%) and sodium borohydride (98%) were purchased from Merck. n-Heptane (HPLC grade, Scharlau) were used without any further purification. Sodium bis(2-ethylhexyl)sulphosuccinate (AOT, 96%) were obtained from ACROS organics. All other chemicals were of analytical grade and used without further purification. All electrochemical experiments were carried out at room temperature. Distilled water was used throughout. The electrochemical experiments were performed in a three-electrode cell arrangement. A platinum sheet of the geometric area of about $20 \, cm^2$ was used as counter electrode, while all potentials were measured with respect to a commercial saturated calomel reference electrode (SCE). Electrochemical experiments were carried out using a Princeton Applied Research, EG&G PARSTAT 2263 Advanced Electrochemical system run by Powersuite software. Morphology, alignment, and composition of the TiO_2 nanotube array and palladium coating on TiO_2 nanotubes matrix were characterized with a scanning electron microscope (Philips, Model XL30) and energy-dispersive X-ray spectroscopy (EDX). To observe photo-enhanced catalysis, cyclic voltammograms of lactose oxidation were obtained with/without UV illumination. A 300 W Hg lamp was used as a UV light source.

2.2. Preparation of titanium oxide nanotubes

Self-organized TiO_2 nanotube arrays on a pure titanium substrate were prepared by anodizing of pure titanium sheet in a non-aqueous fluoride-containing electrolyte. Titanium discs were cut from a titanium sheet (purity 99.99%, 1 mm thickness) and mounted using polyester resin. Titanium samples were degreased by immersion in acetone and ethanol followed by rinsing with distilled water. Anodic films were grown from titanium by anodizing in an ethylene glycol electrolyte containing $25 \times 10^{-4}\%$ (w/v) NH_4F at a constant voltage of 40 V using a platinum sheet as counter
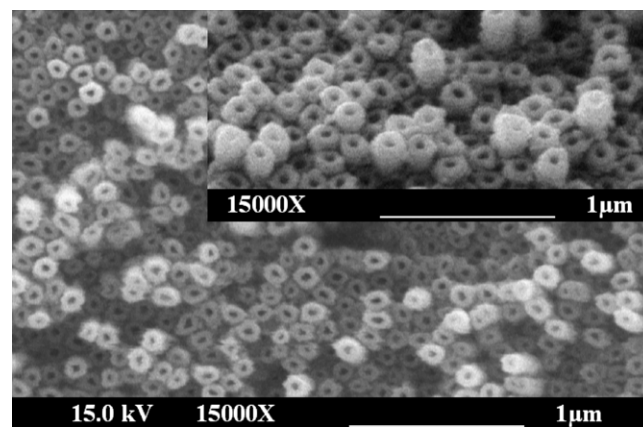
Fig. 1. The surface morphology of the TiO_2 nanotube arrays prepared by anodizing of titanium. (Insert) The surface morphology of Pt/TNTs/Ti electrode.

electrode. The TiO_2 nanotube samples were then annealed at 450 °C in air for 3 h.

2.3. Preparation of Pt/TNT/Ti catalysts

Platinum nanoparticles were produced in a water-in-oil micro-emulsions consisting of n-heptane as the continuous oil phase, AOT as the surfactant and the aqueous solutions of metal precursor or reducing agent. The metal precursor and reducing agent containing micro-emulsions were prepared by mixing the desired amounts of the proper chemicals to obtain micro-emulsions with 15 wt% of surfactant (AOT) and following molar ratios of $[H_2O]/[AOT] = 8$, and aqueous phase concentrations of $[NaBH_4]/[Pt] = 7.5$, $[Pt] = 0.8$ M. For preparation of Pt/TNT/Ti electrodes, at the first, the TiO_2 nanotube samples were ultrasonically cleaned in distilled water for 5–10 min to remove surface contaminants and then were immerged in a solution containing two mentioned mixture. Acetone was used to break the micro-emulsion and precipitate out the platinum nanoparticles on the TiO_2 nanotubes. Finally, Pt/TNTs/Ti electrodes were washed sequentially with n-heptane, acetone and hot distilled water to remove all remaining chemicals. In order to determine how much Pt (mass) is present on the nanotubes, the final platinum loading, as measured by dissolution of the deposit followed by ICP analysis was about $0.9 \, mg \, cm^{-2}$.

3. Results and discussion

3.1. Characterization of the electrodes morphology

Fig. 1 shows scanning electron microscopy (SEM) images of titanium dioxide nanotubes prepared by anodic oxidation and platinum nanoparticles loaded on titanium dioxide nanotubes by micro-emulsion method. The average tube diameter was about 70–90 nm, which can be used as good carrier of particle catalyst and platinum nanoparticles are distributed at the surface of the titanium dioxide nanotubes. Fig. 2 shows the EDX plots of Pt/TNTs/Ti electrodes. EDX results confirm the presence of platinum nanoparticle on the surface TiO_2 nanotubes.

3.2. Characterization of the Pt/TNT/Ti electrode surface

To determine whether the deposition procedure by micro-emulsion method had resulted in the removal of the oxide layer, thereby ensuring good electrical contact between the platinum deposit and TiO_2 nanotubes coating and the underlying titanium electrode, the Pt/TNTs/Ti were tested as electrodes using a one electron redox couple. Fig. 3 shows the voltammetric curves for the
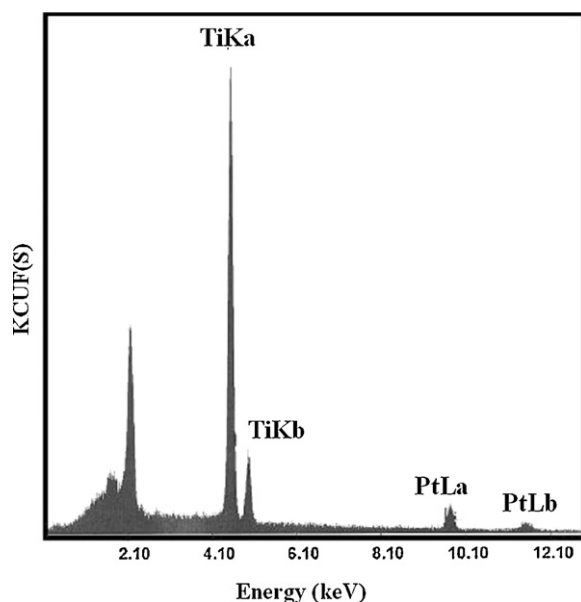
Fig. 2. EDX of Pt/TNT/Ti electrode.

reduction of $K_3Fe(CN)_6$ on Pt/TNT/Ti, smooth platinum and bare TiO$_2$ nanotubes electrodes. The voltammogram for the Pt/TNT/Ti electrode shows the expected reversible behavior for the reduction on a bulk platinum electrode. It suggests that the adhesion and electrical contact of the platinum film with titanium is quite satisfactory. In comparison, the voltammogram obtained with bare TiO$_2$ nanotubes electrode shows increased peak separation and peak widths. This is probably attributable to a passivating surface film, most likely the oxide layer present on the surface of the titanium electrode. This oxide film could grow thicker when using TiO$_2$ nanotubes as an electrode, due to electrochemical (or chemical through ferricyanide) oxidation [41].

3.3. Oxidation of lactose at Pt/TNT/Ti catalyst

In order to find the best medium for oxidation of lactose, the method of cyclic voltammetry was used to estimate the electro-catalytic behavior of Pt/TNT/Ti catalysts in acidic, neutral and alkaline medium. The voltammograms of Pt/TNT/Ti electrode in
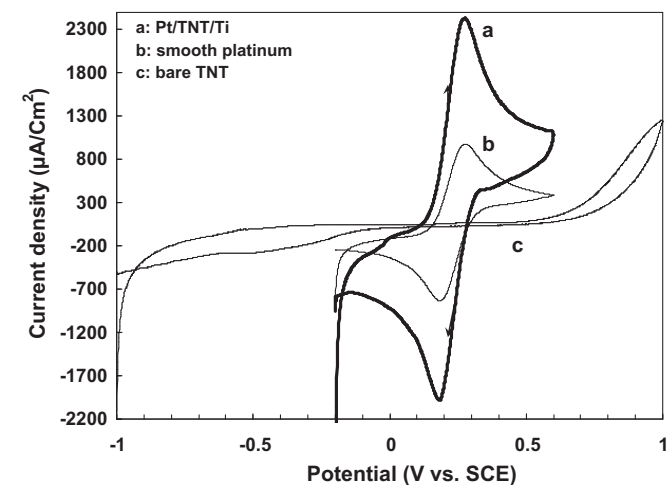

Fig. 3. Cyclic voltammograms for Pt/TNT/Ti (1 cm × 1 cm), smooth platinum (1 cm × 1 cm) and bare TiO$_2$ nanotubes (1 cm × 1 cm) electrodes, recorded at 100 mV s^{-1} in a solution containing 10 mM K$_3$[Fe(CN)$_6$] + 1 M KCl at 25 °C with a scan rate of 100 mV s^{-1}.

presence of 0.01 M lactose in 0.1 M H$_2$SO$_4$, in phosphate buffer (pH 7) and in 0.1 M NaOH are given in Fig. 4A–C. Lactose appears to be very weakly oxidized in 0.1 M H$_2$SO$_4$ and in phosphate buffer medium and the overall current densities increase with an increase of pH. Conversely, the oxidation currents are high in 0.1 M NaOH. Thus, similar to glucose, in alkaline environment the rate of oxidation of lactose is higher than that in acidic and neutral media [42,43].

In order to compare Pt/TNT/Ti electrode with smooth platinum electrode, the method of cyclic voltammetry was used to estimate the electro-catalytic behavior of the electrodes. Fig. 4D shows the comparison of lactose oxidation on smooth platinum electrode and Pt/TNT/Ti electrode. It can be seen from Fig. 4D that the current density for lactose oxidation on Pt/TNT/Ti electrode is greater than that observed for smooth platinum electrode, indicating the surface area of Pt/TNT/Ti electrode was enlarged by dispersion platinum nanoparticles in TiO$_2$ nanotube matrix.

Four oxidation peaks are noticed, three (A$_1$, A$_2$ and A$_3$) during the positive variation of potential and the other (A$_4$), during the negative variation of potential. Peak A$_1$ lies in the hydrogen region. Its position leads to the suggestion that the mechanism for the first oxidation peak of lactose could be similar to that of glucose. According to literatures, the peak A$_1$ at the low potential region is often attributed to the dehydrogenation of lactose on active Pt surface, producing a layer of adsorbed lactose intermediates on electrode surface. These intermediate species were then oxidized at a positive potential, resulting in peaks A$_2$ and A$_3$. Further increasing the potential, surface metal oxides generate which are nearly inactive for lactose oxidation, resulting in a current drop at higher potential. The peak A$_4$ was ascribed to the lactose electro-adsorption on the freshly produced active Pt surface during the negative scan [36,44].

In order to confirm that these peaks (A$_1$, A$_2$ and A$_3$) are not due to the platinum nanoparticles, we performed cyclic voltammograms of Pt/TNT/Ti catalyst in a 0.1 M NaOH aqueous solution at different scan rate and results are presented in Fig. 4E. As can be seen, cyclic voltammograms of Pt/TNT/Ti catalyst in a 0.1 M NaOH aqueous solution exhibited no peaks of A$_2$, A$_3$, and A$_4$, so it can be concluded that the peak A$_2$, A$_3$, and A$_4$ attribute to lactose oxidation.

A further investigation was done to find out the transport characteristics of lactose in Pt/TNT/Ti catalyst. The influence of the scan rate (ν) on the electro-oxidation of lactose the Pt/TNT/Ti catalyst was investigated and shown in Fig. 5. From the figure it can be observed that a straight relationship exists thereby showing that the process of lactose oxidation may be controlled by diffusion. The anodic peak current (peak B) is linearly proportional to $\nu^{1/2}$ as shown in Fig. 5B suggest that the electro-catalytic oxidation of lactose on Pt/TNT/Ti electrode is diffusion-controlled processes.

3.4. Effect of upper limit potentials region

In order to reveal the correlation between lactose oxidation and platinum oxide species, we have studied the effect upper limit potentials (EU) in cyclic potential scanning the lactose oxidation. Fig. 6 shows the cyclic voltammograms of lactose oxidation on the Pt/TNT/Ti electrode for EU of 0.5–0.85 V. As seen in Fig. 6 by creasing the final positive potential limit, the anodic currents of lactose oxidation in the positive going potential sweep (PGPS) remains unchanged (peaks A$_1$, A$_2$ and A$_3$), but oxidation current in the negative going potential sweep (NGPS) is decreased (peak A$_4$). In lower limit potential, the platinum oxides with high valence have not developed greatly, so the effect of the platinum oxides with high valence on lactose oxidation in the NGPS is relatively small. It can be seen that the potential of lactose oxidation peaks remain invariable in the PGPS, while the potential of lactose oxidation peak shifts positively in the NGPS. On the other hand, the peak current in the
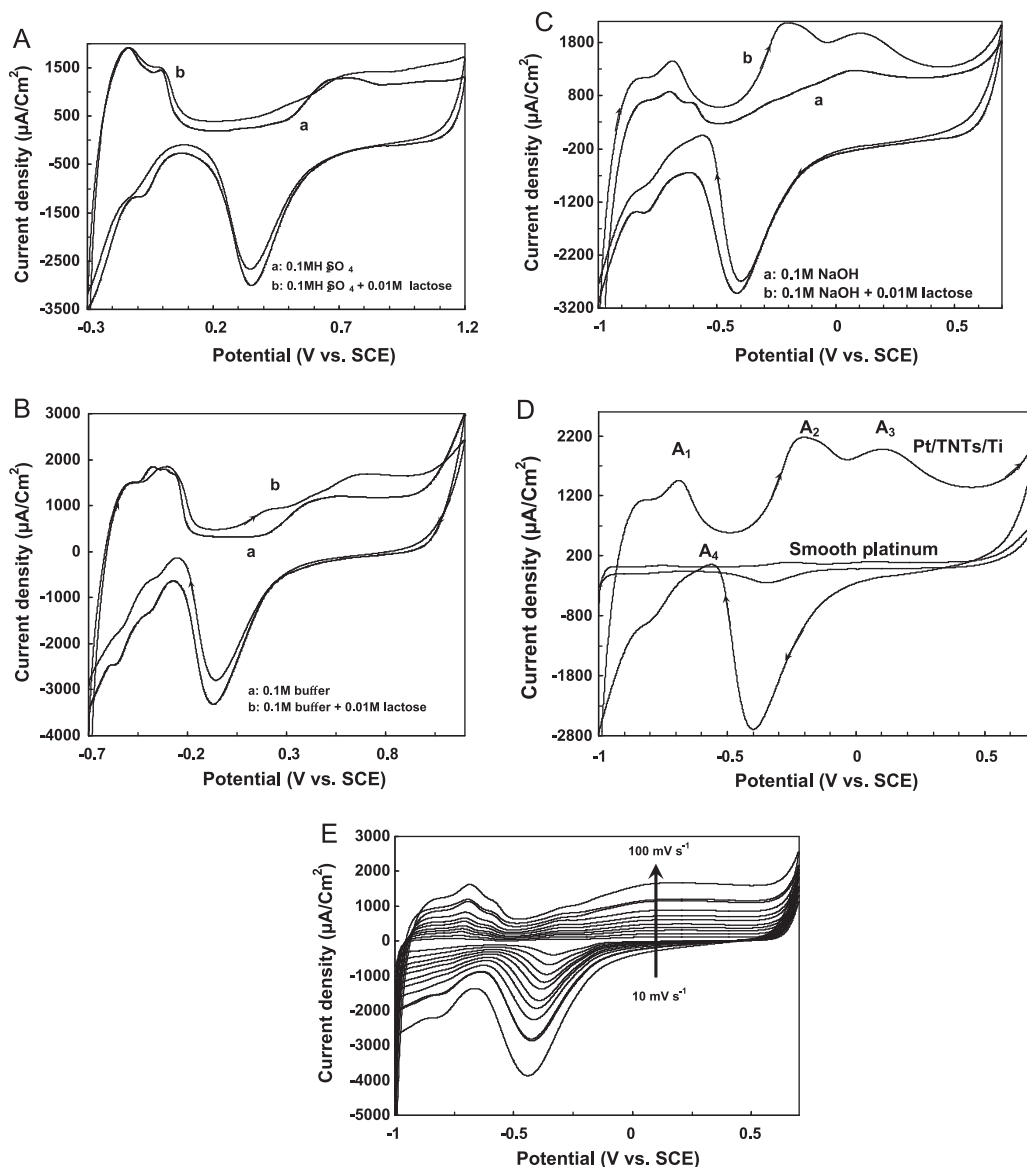
Fig. 4. The cyclic voltammograms of Pt/TNT/Ti catalysts (A) in 0.1 M H$_2$SO$_4$; (B) in phosphate buffer medium (pH 7) and (C) in 0.1 M NaOH, recorded at 100 mV s^{-1}, and at 25 °C, without (a) and with (b) 0.01 M lactose. (D) Cyclic voltammograms for Pt/TNT/Ti and smooth Pt electrodes in a 0.1 M NaOH + 0.01 M lactose aqueous solution at 25 °C with a scan rate of 100 mV s^{-1}. (E) Cyclic voltammograms of Pt/TNT/Ti catalyst in a 0.1 M NaOH aqueous solution at different scan rate.

NGPS decreased as the EU increased. Indeed, by increasing final positive potentials, the conversion of Pt to PtO is accelerated and caused a decrease of oxidation current in the NGPS, which further demonstrates that lactose can only be oxidized on clean metallic platinum nanoparticles surface [45].

### 3.5. Stability of the Pt/TNT/Ti catalyst

In practical view, long-term stability of the electrode is important. The long-term stability of Pt/TNT/Ti was examined in 0.1 M NaOH solution containing 0.01 M lactose (Fig. 7A). It can be observed that the anodic current remains constant with an increase in the scan number at the initial stage and then starts to decrease after 50 scans. The peak current of the 250th scan is about 90% than that of the first scan. In general, the loss of the catalytic activity after successive number of scans may result from the consumption of lactose during the CV scan. It may also be due to poisoning and the structure change of the metal nanoparticles as a result of the perturbation of the potentials during the scanning in aqueous

solutions, especially in presence of the organic compound. Another factor might be due to the diffusion process occurring between the surface of the electrode and the bulk solution. With an increase in scan number, lactose diffuses gradually from the bulk solution to the surface of the electrode [45].

In order to further evaluate the stability of the electro-catalytic activity of the Pt/TNT/Ti catalysts toward lactose, chronoamperometric measurements were performed. Fig. 7B shows the chronoamperometric curves of 0.01 M lactose + 0.1 M NaOH solution on the Pt/TNT/Ti and smooth platinum electrodes at −0.1 V for 300 s, respectively. It was found that the currents observed from chronoamperograms were in good agreement with the currents observed from cyclic voltammetry. On the other hand, as can be seen the current on the Pt/TNT/Ti and smooth platinum electrode decreased with time and reached at 300 s to 1.02 and 0.001 mA, respectively. Compared to the smooth platinum electrode, the relative value of the decrease for the Pt/TNT/Ti is much lower. These results show that the current represent less decay at the applied constant potential on the Pt/TNT/Ti for a long duration (300 s),
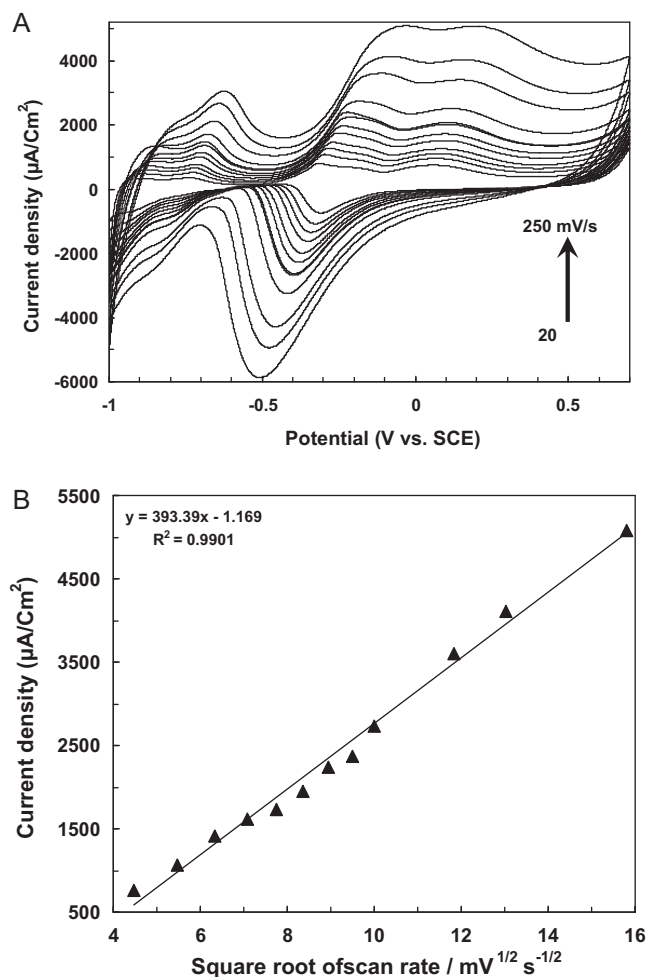
Fig. 5. (A) The cyclic voltammograms of lactose oxidation on Pt/TNT/Ti catalyst in a 0.01 M lactose + 0.1 M NaOH aqueous solution at different scan rate. (B) The dependence of lactose oxidation peak current on the square root of scan rates.
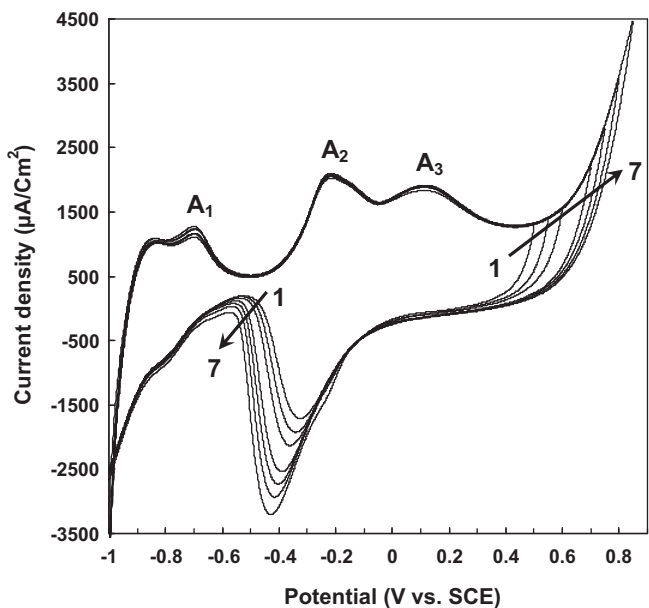
Fig. 6. Effect of upper limit of potential scanning region on the electro-oxidation of 0.01 M lactose on the Pt/TNT/Ti catalyst in 0.1 M NaOH from (1) −1.0 V to 0.5 V to (7) −1.0 V to 0.85 V with a scan rate of 100 mV s^{-1}.
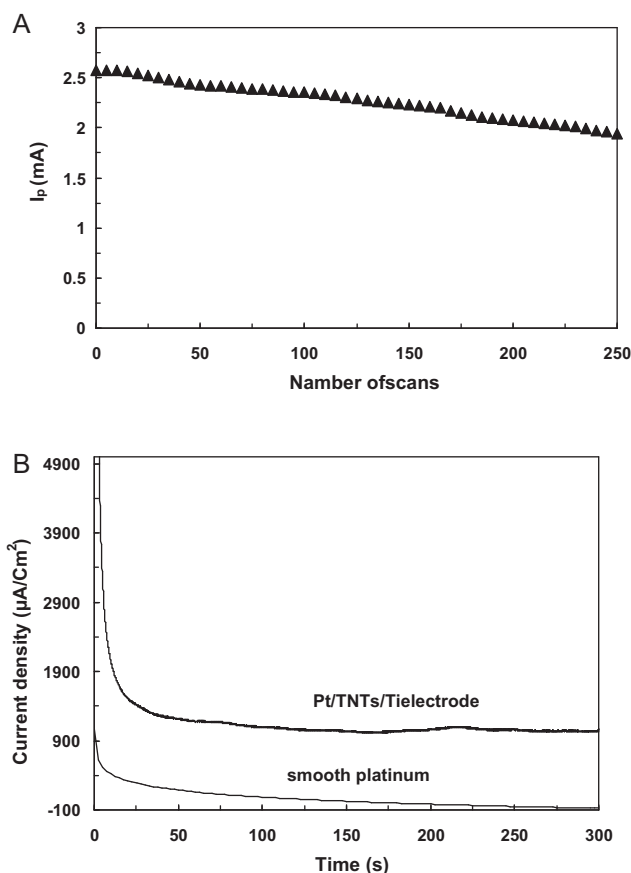

Fig. 7. (A) Plot of anodic peak current in forward scan (A$_3$) in the electro-oxidation of 0.01 M lactose as a function of scan number in cyclic voltammetric method at a scan rate of 100 mV s^{-1}. (B) Chronoamperometric curves in the same condition on the Pt/TNT/Ti and smooth platinum electrodes (B).

indicating that Pt/TNT/Ti exhibits a steady-state electrolysis activity for lactose oxidation.

### 3.6. Photo (UV)-enhanced performance of Pt/TNT/Ti catalyst for lactose oxidation

UV effect on the electrochemical performances of Pt/TNT/Ti catalysts toward lactose oxidation is tested. Fig. 8A shows the cyclic voltammograms of lactose oxidation on Pt/TNT/Ti catalysts in the presence of 0.01 M lactose + 0.1 M NaOH with (a) and without (b) UV illumination, respectively. With the UV light irradiation on the surface of the Pt/TNT/Ti catalyst, the peak current density increases substantially, indicating that the UV light irradiation can remarkably improve the anodic peak current density of lactose oxidation. The peak current density of lactose oxidation on Pt/TNT/Ti catalyst with UV illumination (2.53 mA cm^2) is about 1.7 times of that on Pt/TNT/Ti without UV illumination (1.48 mA cm^2). Such an increased current density of lactose oxidation on the Pt/TNT/Ti catalyst may be attributed to both efficient photo-catalysis and an increased photocurrent of TiO$_2$ under UV illumination.

In order to study of electrochemical performances of lactose on the TNT/Ti electrode under the same conditions, the method of cyclic voltammetry was used to estimate the electro-catalytic behavior of the TNT/Ti electrodes. Fig. 8B shows the cyclic voltammograms of lactose oxidation on TNT/Ti electrode in the presence of 0.01 M lactose + 0.1 M NaOH without (a) and with (b) UV illumination, respectively. As can be seen, TNT/Ti electrode exhibited no oxidation peak for lactose, so TNT/Ti electrodes have not any
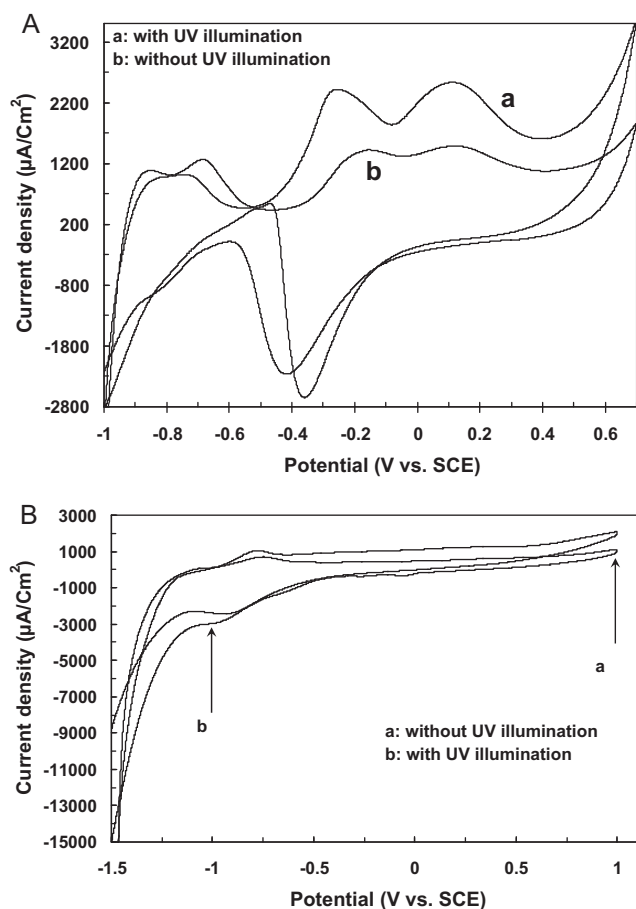
Fig. 8. (A) Cyclic voltammograms of Pt/TNT/Ti catalyst in an aqueous solution of 0.1 M NaOH + 0.01 M lactose with (a) and without (b) UV illumination, respectively. Scan rate was 50 mV s^{-1}. (B) Cyclic voltammograms of TNT/Ti electrode in an aqueous solution of 0.1 M NaOH + 0.01 M lactose without (a) and with (b) UV illumination, respectively.

electro-catalytic activity for lactose oxidation (without UV illumination or with UV illumination). So it can be concluded that the electro-catalytic activity is mainly due to the presence of platinum nanoparticles on TNT/Ti supports.
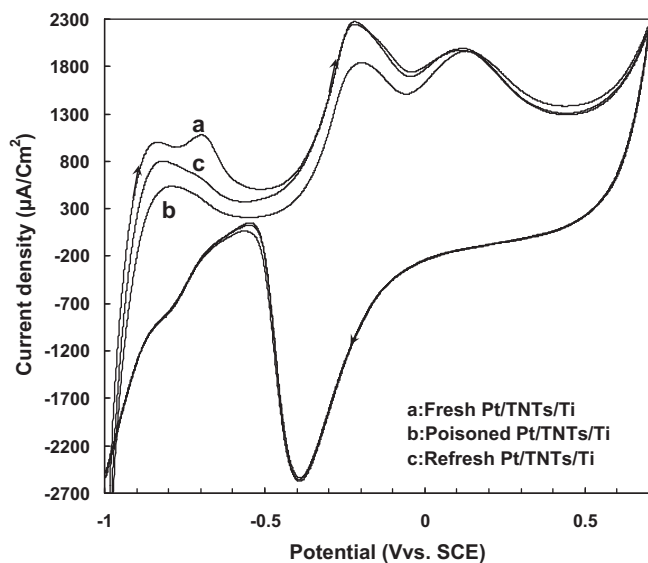
Fig. 9. Voltammetric response of the fresh, poisoned, refresh Pt/TNT/Ti electrode in a 0.1 M NaOH–0.01 M lactose solution at 25 °C with a scan rate of 100 mV s^{-1}.

3.7. Refreshable property of Pt/TNT/Ti catalysts

Platinum is most extensively used catalyst for electro-oxidation of hydrocarbons such as glucose, galactose, and lactose and so on. However, with platinum as an anode catalyst, the surface is usually heavily poisoned by the strong adsorption of intermediates produced during the oxidation of organic fuels, resulting in the lowering of catalytic performance. To resolve such a problem, in the present case the platinum nanoparticles are in close vicinity to TiO$_2$ which, via a photo-catalytic reaction produces a self-cleaning environment [38]. To explore how far this effect can be exploited to refresh the Pt-catalyst, Pt/TNT/Ti catalyst was cycled in the potential range for lactose oxidation namely −0.1 to 0.7 V in alkaline solution for 250 cycles. Fig. 9 shows CV curves of lactose electro-oxidation for a freshly Pt/TNT/Ti electrode, a poisoned Pt/TNT/Ti electrode (after 250 cycles) and after an exposure to UV light. Clearly, the CV curve after UV exposure returns almost fully to its original shape and magnitude.

4. Conclusions

Pt/TNT/Ti catalysts with highly porous structure and excellent electro-catalytic property were prepared by anodizing of titanium sheets followed by doping of platinum nanoparticles with micro-emulsion method. The electrochemical behavior of the Pt/TNT/Ti catalyst was investigated for lactose oxidation reaction in alkaline solution. Pt/TNT/Ti catalyst showed a remarkably enhanced performance for lactose oxidation under UV illumination compared to that without UV illumination. Advantages of using Pt/TNT/Ti catalyst for lactose electro-oxidation is that the high current density and good stability are combined with a strong anti-poisoning ability, i.e. the excellent photo-catalytic properties of TiO$_2$ make the catalyst reusable after a short UV treatment. This study provides a promising route for the simple, facile and cost-effective synthesis of refreshable Pt/TNT/Ti catalyst and the as-synthesized catalysts show great prospect in the applications of direct lactose fuel cell.

References

[1] P. Parpot, V.P. Muiuane, V. Defontaine, A.P. Bettencourt, Electrochim. Acta 55 (2010) 3157–3163.
[2] E. Shoji, M.S. Freund, J. Am. Chem. Soc. 123 (2001) 3383–3384.
[3] T. You, O. Niwa, Z. Chen, K. Hayashi, M. Tomita, S. Hirono, Anal. Chem. 75 (2003) 5191–5196.
[4] L. Wu, X. Zhang, H. Ju, Biosens. Bioelectron. 19 (2007) 141–147.
[5] L. Meng, J. Jin, G. Yang, T. Lu, H. Zhang, C. Cai, Anal. Chem. 81 (2009) 7271–7280.
[6] J.D. Newman, A.P.F. Turner, Biosens. Bioelectron. 20 (2005) 2435–2453.
[7] V. Ganesh, S. Farzana, S. Berchmans, J. Power Sources 196 (2011) 9890–9899.
[8] M.F.L. de Mele, H.A. Videla, A.J. Arvia, Bioelectrochem. Bioenerg. 10 (1983) 239–249.
[9] Yu.B. Vassilyev, O.A. Khazova, N.N. Nikolaeva, J. Electroanal. Chem. 196 (1985) 105–125.
[10] G.G. Neuburger, D.C. Johnson, Anal. Chem. 59 (1987) 150–154.
[11] S.V. Prabhu, R.P. Baldwin, Anal. Chem. 61 (1989) 852–856.
[12] P. Luo, F. Zhang, R.P. Baldwin, Anal. Chim. Acta 244 (1991) 169–178.
[13] J. Ye, R.P. Baldwin, J. Chromatogr. A 687 (1994) 141–148.
[14] R.E. Reim, R.M. Van Effen, Anal. Chem. 58 (1986) 3203–3207.
[15] X. Zhang, K.Y. Chan, A.C.C. Tseung, J. Electroanal. Chem. 386 (1995) 241–243.
[16] J. Wang, Z. Taha, Anal. Chem. 62 (1990) 1413–1416.
[17] B. Beden, F. Largeaud, K.B. Kokoh, C. Lamy, Electrochim. Acta 41 (1996) 701–709.
[18] G. Gao, D. Guo, H. Li, Electrochem. Commun. 9 (2007) 1582–1586.
[19] K.I. Ozoemena, T. Nyokong, Talanta 67 (2005) 162–168.
[20] J. Li, X. Lin, Sens. Actuators B 126 (2007) 527–535.
[21] R. Ganesan, J.S. Lee, J. Power Sources 157 (2006) 217–221.
[22] J. Wang, M. Musameh, Y. Lin, J. Am. Chem. Soc. 125 (2003) 2408–2409.
[23] B. Dong, B.L. He, Y.M. Chai, C.G. Liu, Mater. Chem. Phys. 120 (2010) 404–408.

[24] J.N. Nian, H. Teng, J. Phys. Chem. B 110 (2006) 4193–4198.
[25] P. Hoyer, Langmuir 12 (1996) 1411–1413.
[26] C. Ruan, M. Paulose, O.K. Varghese, G.K. Mor, C.A. Grimes, J. Phys. Chem. B 109 (2005) 15754–15759.
[27] M. Paulose, K. Shankar, S. Yoriya, H.E. Prakasam, O.K. Varghese, G.K. Mor, T.A. Latempa, A. Fitzgerald, C.A. Grimes, J. Phys. Chem. B 110 (2006) 16179–16184.
[28] K. Shankar, G.K. Mor, A. Fitzgerald, C.A. Grimes, J. Phys. Chem. C 111 (2007) 21–26.
[29] Z.H. Zhang, Y. Yuan, Y.J. Fang, L.H. Liang, H.C. Ding, G.Y. Shi, L.T. Jin, J. Electroanal. Chem. 610 (2007) 179–185.
[30] Y. Fu, Z.D. Wei, S.G. Chen, L. Li, Y.C. Feng, Y.Q. Wang, X.L. Ma, M.J. Liao, P.K. Shen, S.P. Jiang, J. Power Sources 189 (2009) 982–987.
[31] M.G. Hosseini, M.M. Momeni, J. Mater. Sci. 45 (2010) 3304–3310.
[32] M.G. Hosseini, M.M. Momeni, M. Faraji, J. Mater. Sci. 45 (2010) 2365–2371.
[33] M.G. Hosseini, M. Faraji, M.M. Momeni, S. Ershad, Microchim. Acta 172 (2011) 103–108.
[34] M.G. Hosseini, M.M. Momeni, M. Faraji, J. Mol. Catal. A: Chem. 335 (2011) 199–204.
[35] M.G. Hosseini, M.M. Momeni, M. Faraji, Electroanalysis 23 (2011) 1654–1662.
[36] H. Druliolle, K.B. Kokoh, B. Beden, Electrochim. Acta 39 (1994) 2577–2584.
[37] C.C. Jia, H.M. Yin, H.Y. Ma, R.Y. Wang, X.B. Ge, A.Q. Zhou, J. Phys. Chem. C 113 (2009) 16138–16143.
[38] L. Hu, K. Huo, R. Chen, B. Gao, J. Fu, P.K. Chu, Anal. Chem. 83 (2011) 8138–8144.
[39] K. Drew, G. Girishkumar, K. Vinodgopal, P.V. Kamat, J. Phys. Chem. B 109 (2005) 11851–11857.
[40] H. Zhang, W. Zhou, Y. Du, P. Yang, C. Wang, J. Xu, Int. J. Hydrogen Energy 35 (2010) 13290–13297.
[41] S.A.G. Evans, J.G. Terry, N.O.V. Plank, A.J. Walton, L.M. Keane, C.J. Campbell, P. Ghazal, J.S. Beattie, T.J. Su, J. Crain, A.R. Mount, Electrochem. Commun. 7 (2005) 125–129.
[42] J. McGinley, F.N. McHale, P. Hughes, C.N. Reid, A.P. McHale, Biotechnol. Lett. 26 (2004) 1771–1776.
[43] C. Paul Wilde, M. Zhang, J. Chem. Soc. Faraday Trans. 89 (1993) 385–389.
[44] X. Yan, X. Ge, S. Cui, Nanoscale Res. Lett. 6 (2011) 313–318.
[45] B. Habibi, N. Delnavaz, Int. J. Hydrogen Energy 36 (2011) 9581–9590.